ACS OMEGA

Open Access

http://pubs.acs.org/journal/acsodf

Article

Preparation of MPN@Zein-PpIX Membrane and Its Antibacterial Properties

Wenhong Zhou,[#] Zhonghao Jiang,[#] Xiao Lin,[#] Yanan Chen, Quanxin Wu, Jia Chen, Feng Zhang, Guolie Xie, Yang Zhang,* Jiantao Lin,* and Ning Guo*

Cite This: *ACS Omega* 2024, 9, 29274−29281

Read Online

ACCESS | Metrics & More | Article Recommendations | Supporting Information

ABSTRACT: For antibacterial purposes, a photothermal and photodynamic antibacterial membrane was prepared through electrospinning. We used zein as the substrate and introduced Protoporphyrin IX (PpIX) into the protein structure. Then, we used electrospinning technology to weave the modified zein into a fiber structure. We finally introduced a metallic polyphenol network (MPN) coating on the fiber surface to form the final membrane: MPN@Zein-PpIX. Then, we investigated the photothermal and photodynamic properties of the membrane and assessed its antibacterial activity with *in vitro* agar plate counting methods. The MPN@Zein-PpIX membrane exhibited good singlet oxygen generation and excellent photothermal conversion. Additionally, it showed good antibacterial capacity *in vitro*, owing to the combination of photothermal and photodynamic properties. Our research provides a simple approach to prepare a multifunctional membrane with excellent antibacterial ability. We used the electrospinning technique to anchor PpIX onto zein to produce a fiber membrane (Zein-PpIX) that can be adhered in situ to improve the biocompatibility of PpIX, and the MPN makes the membrane surface more hydrophilic and more accessible to adhere to biological tissues. The MPN@Zein-PpIX membrane provided new ideas for combining PDT and PTT, and it had great potential for use in the antibacterial application field.

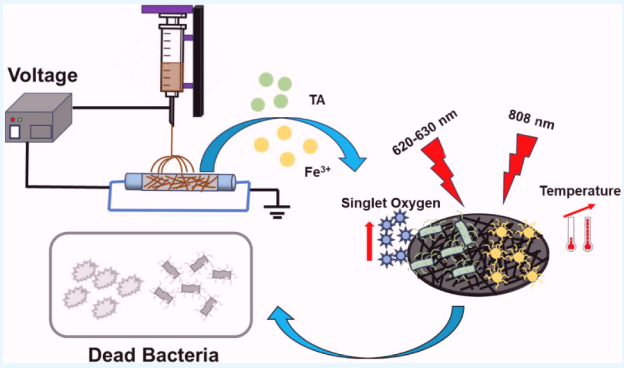

1. INTRODUCTION

Bacterial infection has become one of the top health problems in the world.[1] It can induce many diseases, such as pneumonia, meningitis, sepsis, cholera, skin ulcers, and gastric cancer.[2,3] In particular, the wound is more likely to cause bacterial infection due to the loss of skin protection. Up until now, antibiotics have been the first choice for treating bacterial infections. However, long-term and excessive use of antibiotics may cause severe side effects.[4] Thus, it is imperative to develop more efficient materials with antibacterial capability in a nonantibiotic way.

Photodynamic therapy (PDT) and photothermal therapy (PTT) are two types of light-based local therapies that have attracted increasing attention among many new antibacterial strategies.[5] The PTT technique converts near-infrared radiation (NIR) into heat using photothermal agents, which can kill bacteria by damaging the cell membrane or inactivating essential enzymes and proteins.[6] PTT has many advantages, such as high efficiency, controllability, and limited ability to drug resistance.[7] Therefore, several studies have focused on designing novel photothermal agents to achieve efficient antibacterial activity. The most commonly used photothermal agents are metals, such as Au and pt. For example, Liu et al. combined CeO_2 nanoenzyme with GNRs, which had a good thermal effect. Under 808 nm irradiation, the peroxidase-like activity of the Au complex was significantly enhanced, which made it have a broad-spectrum antibacterial effect.[8,9] PDT is a process that can cause bacterial cell death in the presence of light energy at an appropriate wavelength.[10] Similar to PTT, PDT relies on the involvement of photosensitizers (PSs).[11] The PSs are irradiated with a specific wavelength laser, which excites the PSs to a singlet excited state. However, the excited singlet state has a concise life; it can return to the ground state quickly. The singlet state undergoes intersystem crossing into the excited triplet state to produce a therapeutic effect.[12] During this process, reactive singlet oxygen ($^1O_2$) is produced, which can cause irreversible damage to the main components of bacteria, leading to the death of the bacteria.[13]

With increasing research on PDT and PTT, there are some shortcomings in the current application of PDT and PTT.[14] On the one hand, the production of reactive singlet oxygen

Received: January 6, 2024
Revised: June 2, 2024
Accepted: June 12, 2024
Published: June 27, 2024

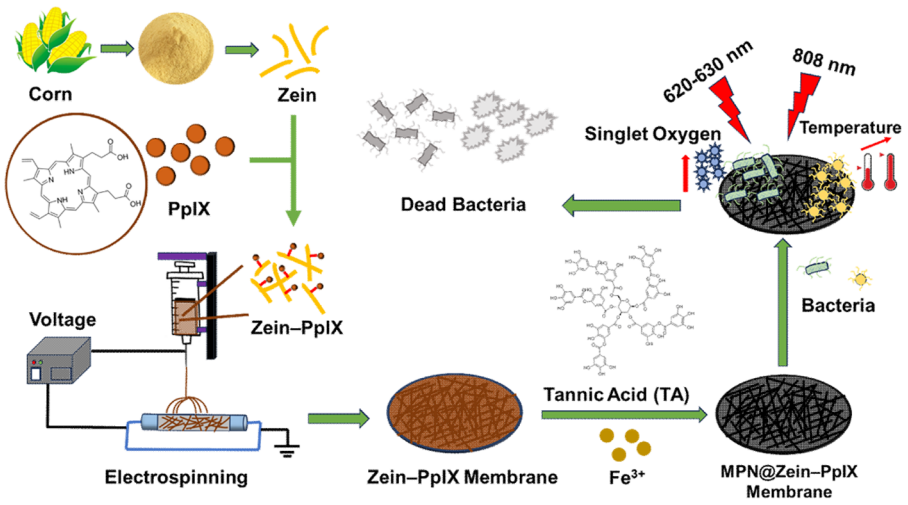

Figure 1. Schematic illustration of the construction of the MPN@Zein-PpIX membrane for combined photothermal and photodynamic antibacterial therapy.

requires oxygen, and many bacterial infections, such as chronic infections, occur in a hypoxic environment. It means that the effect of PDT will decrease in a hypoxic environment.[15] However, the thermal effect generated by PTT has lower specificity in response to bacteria, and the tissue penetration of the specific wavelength laser limits its therapeutic effect.[16] Meanwhile, drugs used for photothermal and photodynamic therapies often exhibit low biocompatibility and difficulty in biodegradation. Furthermore, some new reagents with complex synthesis processes have difficulties in further development.[17]

To overcome the drawbacks caused by the application of PDT or PTT alone, the combination of PDT and PTT has been studied.[18] Protoporphyrin IX (PpIX) is a widely used PS that can produce significant photodynamic effects under the illumination of light sources with 620−630 nm wavelengths.[19] However, free PpIX has poor selectivity and is prone to side effects, such as low biocompatibility and stability.[20] Several studies have proposed methods to modify PpIX to improve its biocompatibility and selectivity and enhance its photodynamic antibacterial effect.[21] In this study, we used the electrospinning technology to anchor PpIX onto zein to produce a fiber membrane (Zein-PpIX) that can be adhered in situ to improve the biocompatibility of PpIX. Zein is the primary storage protein of corn, and it has good biodegradability, good biocompatibility, and nontoxicity. It also has unique film-forming properties. It contains sulfur-containing amino acids that can be connected by disulfide and hydrophobic bonds, facilitating the formation of thin films. Ultimately, zein can form a hard, smooth, hydrophobic, and antibacterial membrane.[22] To achieve the combination of PDT and PTT, we constructed a metal polyphenol network (MPN) on a Zein-PpIX fiber membrane. MPN is a polyphenol network structure formed by chelating the phenol hydroxyl group of polyphenols with metal ions.[23] It acts as a photothermal agent in the photothermal effect. It has excellent photothermal conversion ability, which can convert nearly infrared light energy into heat energy and kill bacteria through thermal damage.[24] In addition, it is easy to synthesize and has good biocompatibility, which has attracted wide attention in the field of antibacterials. In this study, MPN is composed of TA and Fe^{3+}. We used zein as the substrate and introduced PpIX into the protein structure. Then, we used the electrospinning technology to weave the Zein-PpIX into a fiber structure and finally introduced an MPN coating on the fiber surface to form the final membrane: MPN@Zein-PpIX. In this system, zein served as an excellent film-forming polymer material, supporting the photosensitizer PpIX and the photothermal agent MPN. PTT and PDT were combined on one platform, where PpIX produces singlet oxygen and MPN produces a significant thermal effect under different wavelengths of light. Both work together to play the antibacterial role. The MPN@Zein-PpIX membrane provided a new idea for combining PDT and PTT therapies (Figure 1). The experiments indicated that the MPN@Zein-PpIX membrane shows high antibacterial performance and favorable biocompatibility, which ensures the MPN@Zein-PpIX membrane's great potential in clinical applications for antibacterial material.

2. EXPERIMENTAL SECTION

2.1. Materials. Zein was supplied by Macklin (Shanghai, China). PpIX was provided by Shanghai Yuanye Biology Science and Technology Co., Ltd. Vitamin C (Vc), *N*-hydroxysuccinimide (NHS), and *N*-(3-dimethylaminopropyl)-N′-ethylcarbodiimide hydrochloride (EDC·HCl) were purchased from Shanghai Aladdin Biochemical Technology Co., Ltd. The Luria−Bertani (LB) broth, Dulbecco's Modified Eagle Medium (DMEM), and Fetal Bovine Serum (FBS) were obtained from Solarbio Reagent Co., Ltd. (China). Tannic acid (TA) was purchased from Shanghai Aladdin Biochemical Technology Co., Ltd. Iron(III) chloride hexahydrate ($FeCl_3 \cdot 6H_2O$) and Penicillin-Streptomycin Solution were purchased from Innochem Reagent Co, Ltd. (Beijing, China). 1,3-Diphenylisobenzofuran (DPBF, 97%) and 3-(4,5-dimethylthiazol-2-yl)-2,5-diphenyltetrazolium bromide (MTT) were provided by Acros Organics (Shanghai, China). Guangdong Huankai Microbial SCI. and Tech Co., Ltd. (China) supplied us with Mueller Hinton (MH) Agar. Unless otherwise specified, all solvents and chemicals were of analytical grades, and used according to the received standard.

2.2. Synthesis and Characterization of the MPN@Zein-PpIX Membrane. PpIX (0.025 g) and zein (1 g) were separately dissolved in 80% ethanol. Then, EDC·HCl (0.02 g) and NHS (0.02 g) were added to the PpIX solution while being stirred to activate the carboxyl group for 0.5 h. The

https://doi.org/10.1021/acsomega.4c00180
ACS Omega 2024, 9, 29274−29281

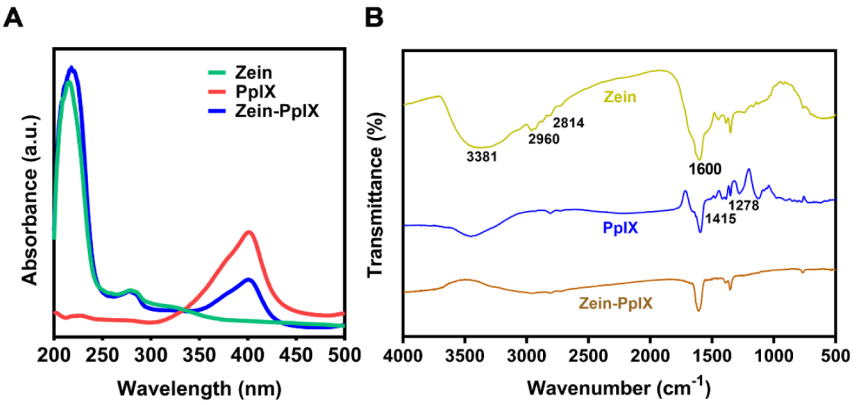

Figure 2. (A) UV−vis spectra of zein, PpIX, and Zein-PpIX. (B) FTIR spectra of zein, PpIX, and Zein-PpIX.

resulting solution was added to the zein solution and stirred overnight. The supernatant was transferred to a dialysis bag (MWCO: 1000 D, MYM Biological Technology Company) and dialyzed against 80% ethanol for 6 h. The resulting product (0.82 g) was obtained through freeze-drying.

To prepare the MPN@Zein-PpIX membrane, Zein-PpIX was dissolved in ethanol for electrospinning. The product was cut into round specimens with a uniform size, shape, and thickness (Φ 10 × 0.2 mm). The sample was then soaked in TA solution (24 mM, 1 mL), and Fe^{3+} solution (4 mM, 0.2 mL) was added gradually to form the TA−Fe^{3+} network. Finally, a black membrane was obtained after drying.

A scanning electron microscope (SEM, Zeiss Gemini SEM 300) was used to observe the morphology and contact angle of the zein, Zein-PpIX, and MPN@Zein-PpIX membranes. The UV−vis absorption was recorded with a UV−visible spectrophotometer (UV-6000PC, Shanghai Metash Instruments Co., Ltd.). Fourier-transformed infrared (FTIR) spectra were obtained by the KBr pellet method with an FTIR spectrophotometer (Bruker, TENSOR 27, Germany). ^{1}H NMR spectra were obtained by nuclear magnetic resonance (NMR) spectroscopy (Bruker 400M, Bruker, Germany).

2.3. Photothermal Properties. The photothermal conversion ability of the membranes was monitored by continuous irradiation. Briefly, zein, Zein-PpIX, and MPN@Zein-PpIX membranes (Φ 10 × 0.2 mm) were immersed in 0.5 mL of water in a 24-well plate. They were irradiated under an 808 nm NIR laser (0.75 W·cm^{-2}) irradiation (Zhongjiao Jinyuan Technology, 16 Ltd., Beijing, China) for 10 min, respectively. Temperature changes were recorded by using an infrared thermal camera. To investigate the effect of laser power on MPN@Zein-PpIX membrane, the sample (Φ 10 × 0.2 mm) was immersed in 0.5 mL water in a 24-well plate and irradiated under an 808 nm NIR laser with different power (0.25/0.5/0.75/1 W·cm^{-2}). To test its photothermal stability, the MPN@Zein-PpIX membrane was exposed to 808 nm laser light (0.5 W·cm^{-2}) for 10 min and cooled to room temperature naturally. The process was repeated in four cycles, and the temperature changes were measured by an infrared thermal camera.

2.4. Detection of $^1O_2$ Generation. DPBF was used as a probe to detect the production of $^1O_2$, and it can react with $^1O_2$, resulting in a decrease in the absorption peak at 410 nm.[25] The Zein-PpIX and MPN@Zein-PpIX membranes (Φ 10 × 0.2 mm) were added to DPBF/acetonitrile solution (0.04 mM, 2 mL) with or without Vc solution (0.5 mg/mL) and irradiated under 620−630 nm LED light for 10 min. The Vc was used as the ROS scavenger. The absorbance spectrum was measured every two minutes. In addition, the same membranes were measured in a DPBF/acetonitrile solution under dark treatment.

2.5. Bacteria Culture. *Staphylococcus aureus* (*S. aureus*, ATCC 25923) and *Escherichia coli* (*E. coli*, ATCC 25922) were generously provided by Guangzhou Institute of Microbiology. The single colony of bacteria was selected from an agar plate and suspended in LB medium. After incubating at 37 °C under 110 rpm shaking for 12 h, the logarithmic growth bacteria were obtained by centrifugation and resuspended in fresh LB medium.

2.6. *In Vitro* Antibacterial Tests. The antibacterial activities of the MPN@Zein-PpIX membrane were evaluated with *E. coli* and *S. aureus* as model bacteria. The MPN@Zein-PpIX membrane (Φ 10 × 0.2 mm) was placed at the bottom of 48-well plates, and 0.5 mL of the bacterial suspension (10^8 CFU) was added to each plate. The samples were then incubated in a shaker at 37 °C and 110 rpm for 3 h to facilitate bacterial adhesion. Next, the suspension was removed, and the free bacteria on the membrane surface were washed away with a NaCl solution (0.9%). Then, 100 μL of NaCl solution (0.9%) was added to the MPN@Zein-PpIX membrane surface, and the samples were irradiated with an 808 nm NIR laser or LED light. The PTT group was irradiated with an 808 nm laser (0.5 W·cm^{-2}) for 5 min. The PDT group was irradiated with LED light (620−630 nm) for 30 min. PTT and PDT groups were subjected to simultaneous irradiation with an 808 nm NIR laser (0.5 W·cm^{-2}) for 5 min and LED light (620−630 nm) for 30 min. The control group was not subjected to light treatment. After irradiation, the MPN@Zein-PpIX membrane was placed in a 1 mL 0.9% NaCl solution and ultrasonicated for 3 min to free the attached bacteria. After treatment, 10 μL of bacterial solution was diluted 10^3 times with 0.9% NaCl and coated on MH solid agar plates to culture overnight at 37 ∘C. Finally, the number of colonies (*CFU*) was counted, and the bacteriostatic rate was according to the following formula:

$$\text{Bacteriostatic rate}(\%) = (CFU_c - CFU_s)/CFU_c \times 100\% \quad (1)$$

where CFU_s represent the number of colonies treated with the MPN@Zein-PpIX membrane under light, and CFU_c is without light.

2.7. *In Vitro* Cytotoxicity Assays. The MTT assay was used to measure the cytotoxicity of the MPN@Zein-PpIX membrane.[26] The mouse fibroblast cells (L929) were used to

https://doi.org/10.1021/acsomega.4c00180
ACS Omega 2024, 9, 29274−29281

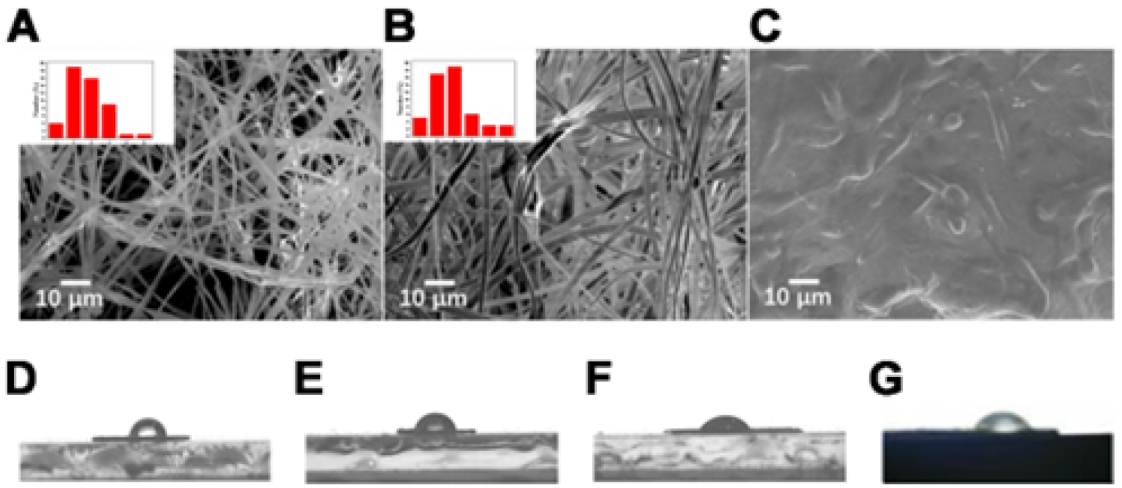

Figure 3. SEM images of (A) zein, (B) Zein-PpIX, and (C) MPN@Zein-PpIX membranes. The small images in the picture represent the statistical result of the diameter of the corresponding fiber membrane. Contact angles of (D) zein, (E) Zein-PpIX, (F) MPN@Zein-PpIX, and (G) MPN.

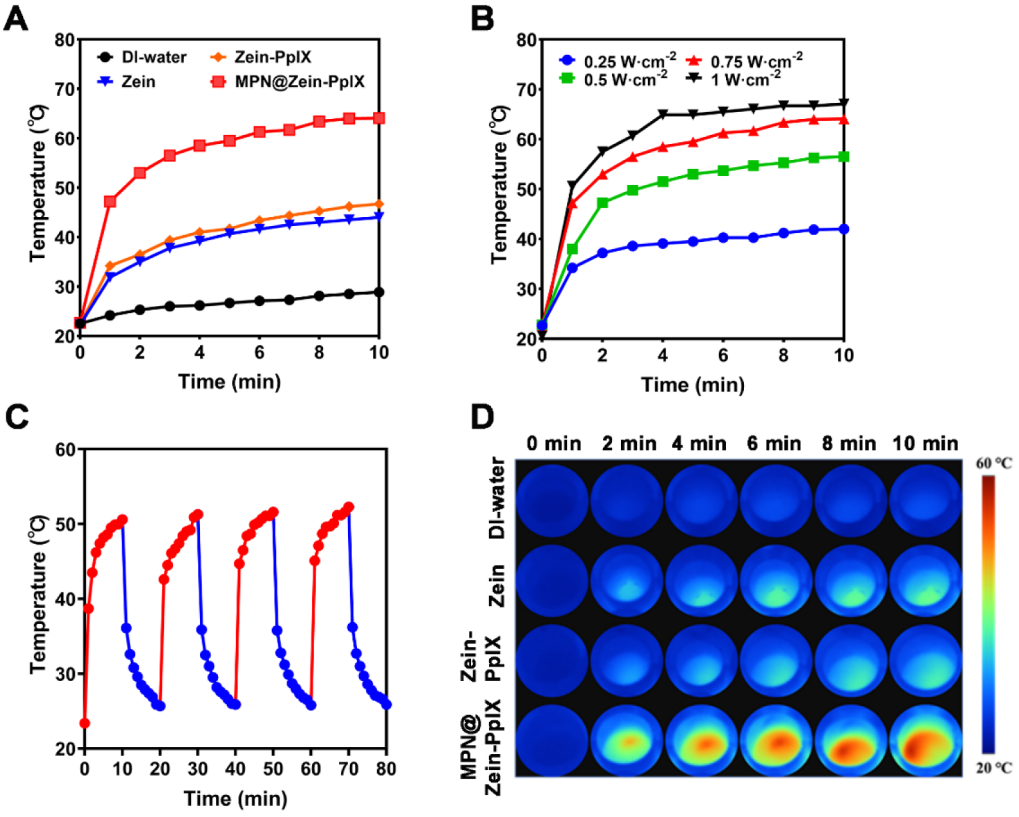

Figure 4. (A) Photothermal curve of zein, Zein-PpIX, and MPN@Zein-PpIX membrane under 808nm NIR (0.75 W·cm^{-2}). (B) Photothermal curve of MPN@Zein-PpIX membrane under an 808 nm NIR (0.25/0.5/0.75/1 W·cm^{-2}). (C) The photothermal curve of the MPN@Zein-PpIX membrane with four irradiation on/off cycles. (D) Photothermal images of DI−water, zein, Zein-PpIX, and MPN@Zein-PpIX membrane.

assess the cell biocompatibility of the MPN@Zein-PpIX membrane, which were obtained from Guangzhou Medical University (Guangdong, China). Briefly, L929 cells (10^4) were first grown in DMEM supplemented with 10% FBS and 1% penicillin/streptomycin. The MPN@Zein-PpIX and zein membranes were incubated with L929 cells in a 96-well plate at 37 °C in a 5% CO_2 atmosphere for 24 and 48 h, respectively. The light groups were irradiated differently (LED: 620−630 nm, 808 nm laser, and LED + 808 nm laser). Next, 10 μL of MTT (5 mg/mL) was added to each well and incubated for another 4 h. The supernatant was removed carefully, following the addition of DMSO (100 μL) to each well along with a 15 min incubation and shaking. The relative cell viability was calculated after measuring the absorbance at 570 nm. Three parallel experiments were conducted for each group, and the cell viability rate was calculated according to the following formula:

$$\text{Viability rate}(\%) = (A_s - A_b)/(A_c - A_b) \times 100\% \quad (2)$$

https://doi.org/10.1021/acsomega.4c00180
ACS Omega 2024, 9, 29274−29281

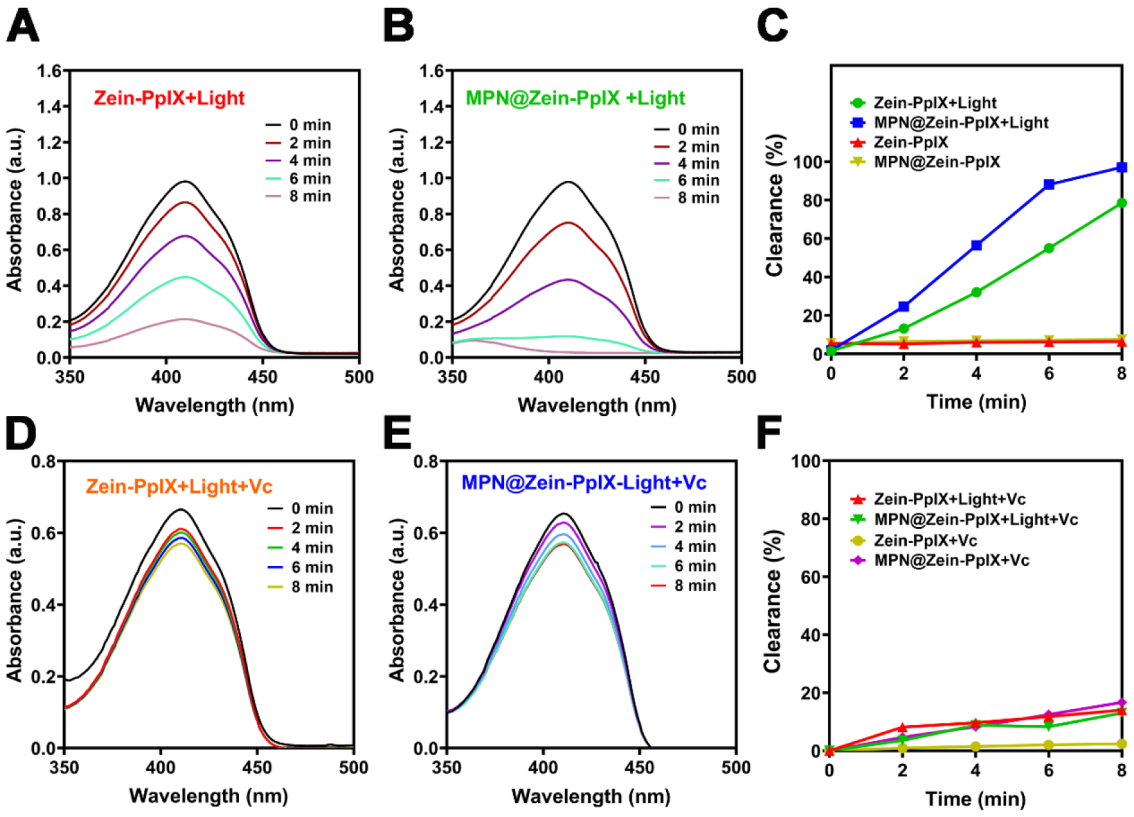

Figure 5. UV−Vis absorption spectra of DPBF solution photo-oxidized at different times by (A) zein−PpIX with light, (B) MPN@Zein−PpIX with light, and (C) Summary of the changes in the clearance of the DPBF solution incubated with Zein-PpIX and MPN@Zein-PpIX with or without irradiation at 410 nm. (D) Zein-PpIX with light and Vc. (E) MPN@Zein-PpIX with light and Vc. (F) Summary of the changes in the clearance of the DPBF solution incubated with Zein-PpIX and MPN@Zein-PpIX with Vc and with or without irradiation at 410 nm.

where A_s is the absorbance of cells treated with zein or the MPN@Zein-PpIX membrane, A_c is the absorbance of cells treated with PBS, and A_b is the absorbance of solution treated without cells and membranes.

2.8. Statistical Analysis. All the results were reported as mean ± SD. The differences among groups were determined using one-way ANOVA analysis and Student's t test: * $p < 0.05$, ** $p < 0.01$, *** $p < 0.001$.

3. RESULTS AND DISCUSSION

3.1. Synthesis and Characterization of the MPN@Zein-PpIX Membrane. Zein was first connected with PpIX by an amido bond to obtain Zein-PpIX, which was dissolved in ethanol for electrospinning. The UV−vis spectrum showed that Zein-PpIX exhibited characteristic absorption peaks of PpIX, indicating that zein and PpIX were successfully connected (Figure 2A). Based on UV−vis analysis, the conjugation ratio of PpIX was calculated to be 2.4%. We further characterized Zein-PpIX by FTIR and ^{1}H NMR (Figures 2B, S1, and S2). FTIR showed that zein included a broad peak at 3381 cm^{-1} due to the stretching of the N-H group. The peaks at 2960 cm^{-1} and 2814 cm^{-1} indicated aliphatic C—H stretching bands.[27] The sharp peak of zein at 1600 cm^{-1} represented amide I on the peptide groups, which is the characteristic vibrational band of zein. In addition, 1415 cm^{-1} was the C—N stretching vibration peak on the pyrrole ring of PpIX. 1278 cm^{-1} was the stretching vibration peak of C—O, which was also the internal vibration of the porphyrin ring. The stretching vibration peak of C—O at 1278 cm^{-1} was decreased in Zein-PpIX, and all peaks were shifted to higher frequencies, which may be due to the reaction between the carboxyl group on the porphyrin ring and the amino group of zein. Due to the introduction of the porphyrin ring, the zein amide band at 1600 cm^{-1} shifted to 1608 cm^{-1}. These changes demonstrated the interaction between zein and PpIX[28] (Figure 2B).

The resultant Zein-PpIX fiber membrane was immersed in the TA solution, and the MPN coating was formed after adding Fe^{3+} solution. SEM was used to observe the membrane morphology and diameter distribution (Figure 3A−3C). Zein and Zein-PpIX fibers exhibited a smooth, uniform, and homogeneous morphology. The average diameters of zein and Zein-PpIX ranged from 2 to 4 μm (Figure 3A, 3B). After being coated with MPN, the membrane became rough. The average diameter of MPN@Zein-PpIX increased to 5 μm, and the bottom was covered because of the increased density of the MPN (Figure 3C). Zein has unique solubility, i.e., it cannot dissolve in water or anhydrous alcohol but dissolves in alcohol aqueous solutions with a volume fraction of 60−95%. Therefore, the zein and Zein-PpIX fiber membranes had larger contact angles (zein: 51.8°; Zein-PpIX: 45.0°), indicating that they exhibit hydrophobicity (Figure 3D, 3E). However, after coating with MPN, the contact angle of MPN@Zein-PpIX decreased to 36.5°, similar to MPN's (36.8°) (Figure 3F, 3G), which was due to the phenolic hydroxyl groups in the polyphenol structure.

3.2. Photothermal and Photodynamic Behaviors of the MPN@Zein-PpIX Membrane. We investigated the photothermal conversion properties after introducing the MPN coating on the Zein-PpIX fiber membrane. As shown

https://doi.org/10.1021/acsomega.4c00180
ACS Omega 2024, 9, 29274−29281

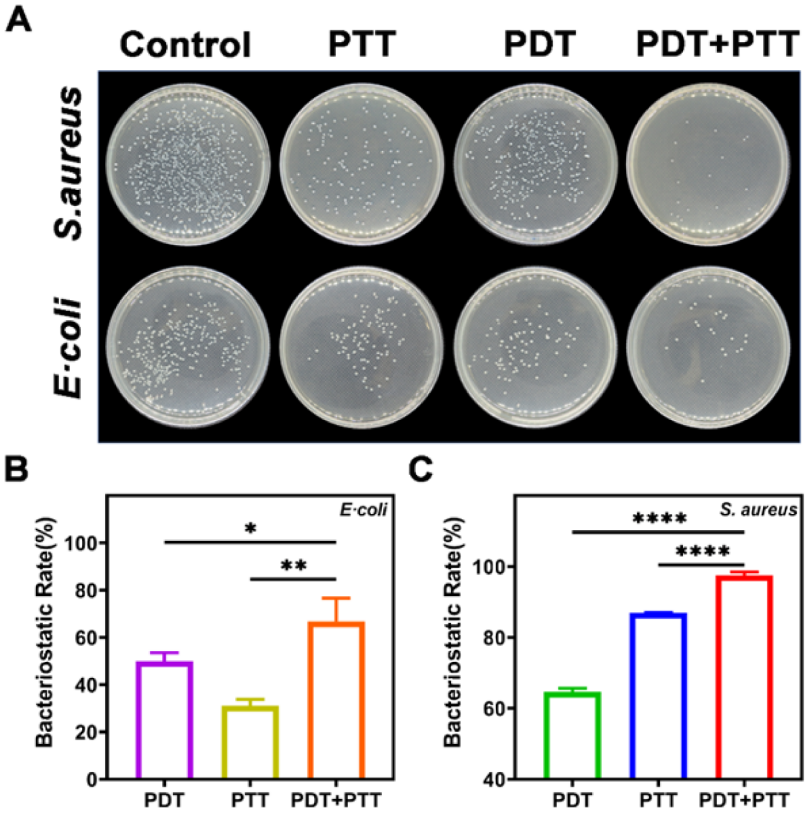

Figure 6. Antibacterial effect of the MPN@Zein-PpIX membrane against *S. aureus* and *E. coli* was evaluated by the (A) agar plate counting method. The bacteriostatic rate against (B) *E. coli* and (C) *S. aureus* was measured according to the results.

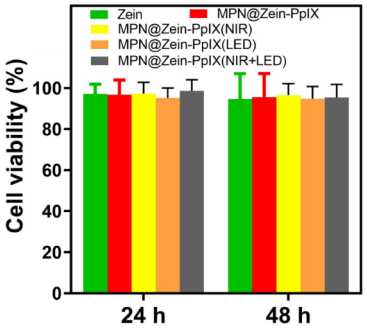

Figure 7. Cytotoxicity of zein and the MPN@Zein-PpIX membrane with or without different light sources.

in Figure 4A–4D, the temperature of MPN@Zein-PpIX membranes increased to approximately 60 °C after irradiating with an 808 nm laser (0.75 W·cm^{-2}, 10 min). In comparison, zein and Zein-PpIX fiber membranes without MPN coating exhibited more minor temperature changes under the same conditions of illumination. So, the MPN coating endowed the Zein-PpIX fiber membrane with excellent photothermal conversion properties. To investigate the effect of laser power on the MPN@Zein-PpIX membrane, we studied the temperature effect of the MPN@Zein-PpIX membrane at different power levels. The temperature of the MPN@Zein-PpIX membrane increases with the increase of laser power (Figure 4B). However, we need to choose a suitable temperature that can effectively kill bacteria without causing too much harm or pain to the human body. Therefore, we ultimately decided to use a laser power of 0.5 W·cm^{-2} throughout the entire experiment. Subsequently, we investigated the photothermal conversion stability of the MPN@Zein-PpIX membrane with multiple cycles of the light cooling process. As shown in Figure 4C, the water temperature around the sample kept increasing to 50 °C after the laser was switched on and off for four circles. The photothermal conversion ability of the MPN@Zein-PpIX membrane can be demonstrated stably.

Besides, because of the presence of PpIX, the MPN@Zein-PpIX membrane could generate singlet oxygen.[29] This ability of the MPN@Zein-PpIX membrane to generate singlet oxygen was measured in the presence of the ROS indicator, DPBF. DPBF possesses high specificity for singlet oxygen and can form inner peroxides to decompose into 1,2-dibenzoylbenzene. Once combined with singlet oxygen, DPBF is irreversibly oxidized, and its absorption intensity decreases rapidly at UV–visible light (410 nm).[30] The more singlet oxygen, the greater the decrease in the absorption intensity. And the higher the clearance of DPBF, the higher the efficiency of ROS production. After LED irradiation (620–630 nm), the absorbance of DPBF in the Zein-PpIX group and the MPN@Zein-PpIX group showed a time-dependent reduction (Figure 5A, 5B). After 6 min of LED irradiation, the DPBF clearances of the Zein-PpIX group and MPN@Zein-PpIX group were 55.1% and 88.2%, respectively. After 8 min of LED irradiation, the DPBF clearances of the Zein-PpIX group and MPN@Zein-PpIX group were 78.6% and 97.2%, respectively. These results indicated that within 8 min of LED irradiation, the ROS generation efficiency of the MPN@Zein-PpIX group was higher than that of the Zein-PpIX group (Figure 5C). Thus, the MPN coating did not weaken singlet oxygen generation by PpIX. In addition, the generation of singlet oxygen relied on the LED light of 620–630 nm because it

https://doi.org/10.1021/acsomega.4c00180
ACS Omega 2024, 9, 29274–29281

showed that the clearance of DPBF did not change in the absence of LED light irradiation. To further confirm the production of singlet oxygen, we conducted experiments using vitamin C as a reactive oxygen species scavenger. Only a small reduction of the absorbance was observed in the presence of irradiation and vitamin C when the DPBF incubated with Zein-PpIX and MPN@Zein-PpIX (Figure 5D, 5E), and after 8 min, the DPBF clearances of Zein-PpIX and MPN@Zein-PpIX were only 14.1% and 13.0%, respectively (Figure 5F). The results showed that vitamin C effectively cleared away the singlet oxygen produced by PpIX, which proved that the MPN@Zein-PpIX membrane can produce singlet oxygen to play the role of PDT. Overall, the MPN@Zein-PpIX membrane provides photodynamic and photothermal properties with different wavelengths of light.

3.3. *In Vitro* Antibacterial Assay. The antibacterial properties of the MPN@Zein-PpIX membrane were assessed by using the agar plate counting method. After incubation with the MPN@Zein-PpIX membrane, *S. aureus* and *E. coli* were treated with 808 nm NIR and 620−630 nm LED light irradiation, respectively, or both types of irradiation (Figure 6A). Owing to the presence of PpIX, the sample showed PDT ability, achieving a bacteriostatic rate of 64.6% (*S. aureus*) and 49.9% (*E. coli*). In addition, the MPN-based photothermal conversion properties allowed the sample to achieve a bacteriostatic rate of 86.9% (*S. aureus*) and 31.1% (*E. coli*) (Figure 6B, 6C). After treatment using the two types of irradiations, the antibacterial effects of the MPN@Zein-PpIX membrane were significantly enhanced. The bacteriostatic rate increased to 97.5% (*S. aureus*) and 66.8% (*E. coli*) with the combination of PDT and PTT (Figures 6B, 6C). In summary, conducting only PDT or PTT could prove significantly disadvantageous for antimicrobial therapy, especially in the case of *E. coli*. However, the synergistic effect of the combination of PTT and PDT can cause damage to bacteria, eventually resulting in bacterial death, because of the simultaneous use of singlet oxygen and high temperature.

3.4. *In Vitro* Biocompatibility Assay. We used the MTT assay to evaluate the in vitro biocompatibility of the MPN@Zein-PpIX membrane. As shown in Figure 7, after incubation with Zein or the MPN@Zein-PpIX membrane for 24 and 48 h, the cell viability in both groups was above 90%, which indicates that the MPN@Zein-PpIX membrane has no potential cytotoxicity to L929 cells. The zein showed a similar trend to MPN@Zein-PpIX membrane, indicating that zein is a safe material and the addition of PpIX and MPN has no significant effect on its biocompatibility. In addition, the survival rate of L929 cells also reached more than 90% under different light sources, indicating that the MPN@Zein-PpIX membrane can maintain its biocompatibility during PDT and PTT.

4. CONCLUSIONS

This study proposed a membrane MPN@Zein-PpIX, which combines PDT and PTT as an antibacterial agent. It combines the photosensitizer PpIX with the photothermal conversion agent MPN, and the synthesis method is very simple. Under different wavelengths of light, the membrane exhibited excellent capabilities for singlet oxygen generation and *in vitro* photothermal conversion. Due to the combination of PDT and PTT, the in vitro antibacterial experiments showed that the MPN@Zein-PpIX membrane had an excellent antibacterial effect on plankton bacteria. Furthermore, *in vitro* cytotoxicity experiments proved that the MPN@Zein-PpIX membrane demonstrates excellent biosafety and is expected to be used as an efficient antibacterial dressing.

■ ASSOCIATED CONTENT

Supporting Information

The Supporting Information is available free of charge at https://pubs.acs.org/doi/10.1021/acsomega.4c00180.

FTIR spectra of physical mixture of zein and PpIX, and Zein-PpIX (Figure S1); the ^{1}H NMR spectra of zein, PpIX, and Zein-PpIX (Figure S2) (PDF)

■ AUTHOR INFORMATION

Corresponding Authors

Yang Zhang − *South China Institute of Collaborative Innovation, Dongguan 523000, China; Guangdong Dongguan Quality Supervision Testing Center, Dongguan 523000, China*; Email: zyxx2010@163.com

Jiantao Lin − *The First Dongguan Affiliated Hospital; School of Pharmacy, Guangdong Medical University, Dongguan 523000, China*; orcid.org/0000-0002-0876-0333; Email: linjt326@163.com

Ning Guo − *The First Dongguan Affiliated Hospital; School of Pharmacy, Guangdong Medical University, Dongguan 523000, China*; orcid.org/0000-0001-5305-5636; Email: guoning0501@hotmail.com

Authors

Wenhong Zhou − *The First Dongguan Affiliated Hospital; School of Pharmacy, Guangdong Medical University, Dongguan 523000, China*; orcid.org/0009-0004-7155-6919

Zhonghao Jiang − *The First Dongguan Affiliated Hospital; School of Pharmacy, Guangdong Medical University, Dongguan 523000, China*

Xiao Lin − *The First Dongguan Affiliated Hospital; School of Pharmacy, Guangdong Medical University, Dongguan 523000, China*

Yanan Chen − *The First Dongguan Affiliated Hospital; School of Pharmacy, Guangdong Medical University, Dongguan 523000, China*

Quanxin Wu − *The First Dongguan Affiliated Hospital; School of Pharmacy, Guangdong Medical University, Dongguan 523000, China*

Jia Chen − *The First Dongguan Affiliated Hospital; School of Pharmacy, Guangdong Medical University, Dongguan 523000, China*

Feng Zhang − *The First Dongguan Affiliated Hospital; School of Pharmacy, Guangdong Medical University, Dongguan 523000, China*

Guolie Xie − *The First Dongguan Affiliated Hospital; School of Pharmacy, Guangdong Medical University, Dongguan 523000, China*

Complete contact information is available at: https://pubs.acs.org/10.1021/acsomega.4c00180

Author Contributions

#W.Z., Z.J., and X.L. contributed equally to this work. Conceptualization: Y.Z., J.L., and N.G.; methodology: W.Z., Z.J., and X.L.; investigation: W.Z., Z.J., X.L., Y.C., Q.W., J.C., F.Z., and G.X.; data curation, W.Z.,Z.J., and X.L., Y.C.; writing−original draft preparation: W.Z., J.L., and N.G.; writing−review and editing: Y.Z., J.L., and N.G.; supervision:

https://doi.org/10.1021/acsomega.4c00180
ACS Omega 2024, 9, 29274−29281

Y.Z., J.L., and N.G.; project administration: W.Z., J.L., and N.G.; funding acquisition: Y.Z., J.L., and N.G. All authors have read and agreed to the published version of the manuscript.

Funding

This research was financially supported by the Innovation Program of Zhanjiang (2020LHJH005), Guangdong Basic and Applied Basic Research Foundation (2020A1515110344, 2023A1515140078), and the National Natural Science Foundation of China (81803723).

Notes

The authors declare no competing financial interest.

REFERENCES

(1) McEwen, S.; Collignon, P. Antimicrobial Resistance: a One Health Perspective. *Microbiol. Spectrum.* **2017**, *6* (11), 255−260.
(2) Ding, Y.; Yuan, Z.; Hu, J.-W.; Xu, K.; Wang, H.; Liu, P.; Cai, K.-Y. Surface modification of titanium implants with micro−nano-topography and NIR photothermal property for treating bacterial infection and promoting osseointegration. *Rare Met.* **2022**, *41* (2), 673−688.
(3) Nataraj, B. H.; Mallappa, R. H. Antibiotic Resistance Crisis: An Update on Antagonistic Interactions between Probiotics and Methicillin-Resistant Staphylococcus aureus (MRSA). *Curr. Microbiol.* **2021**, *78* (6), 2194−2211.
(4) Edwards, F.; MacGowan, A.; Macnaughton, E. Antibiotic resistance. *Medicine* **2021**, *49* (10), 632−637.
(5) Liu, H.; Xing, F.; Zhou, Y.; Yu, P.; Xu, J.; Luo, R.; Xiang, Z.; Rommens, P. M.; Liu, M.; Ritz, U. Nanomaterials-based photothermal therapies for antibacterial applications. *Mater. Design.* **2023**, *233*, 112231.
(6) Qi, X.; Xiang, Y.; Cai, E.; Ge, X.; Chen, X.; Zhang, W.; Li, Z.; Shen, J. Inorganic−organic hybrid nanomaterials for photothermal antibacterial therapy. *Coord. Chem. Rev.* **2023**, *496*, 215426.
(7) Wang, B.; Xu, Y.; Shao, D.; Li, L.; Ma, Y.; Li, Y.; Zhu, J.; Shi, X.; Li, W. Inorganic nanomaterials for intelligent photothermal antibacterial applications. *Front Bioeng. Biotechnol.* **2022**, *10*, 1047598.
(8) Ahmadian, Z.; Gheybi, H.; Adeli, M. Efficient wound healing by antibacterial property: Advances and trends of hydrogels, hydrogel-metal NP composites and photothermal therapy platforms. *J. Drug Delivery Sci. Technol.* **2022**, *73*, 103458.
(9) Chen, Y.; Gao, Y.; Chen, Y.; Liu, L.; Mo, A.; Peng, Q. Nanomaterials-based photothermal therapy and its potentials in antibacterial treatment. *J. Controlled Release* **2020**, *328*, 251−262.
(10) Correia, J. H.; Rodrigues, J. A.; Pimenta, S.; Dong, T.; Yang, Z. Photodynamic Therapy Review: Principles, Photosensitizers, Applications, and Future Directions. *Pharmaceutics* **2021**, *13* (9), 1332.
(11) Ng, X. Y.; Fong, K. W.; Kiew, L. V.; Chung, P. Y.; Liew, Y. K.; Delsuc, N.; Zulkefeli, M.; Low, M. L. Ruthenium(II) polypyridyl complexes as emerging photosensitisers for antibacterial photodynamic therapy. *J. Inorg. Biochem.* **2024**, *250*, 112425.
(12) Amos-Tautua, B. M.; Songca, S. P.; Oluwafemi, O. S. Application of Porphyrins in Antibacterial Photodynamic Therapy. *Molecules* **2019**, *24* (13), 2456.
(13) Sabino, C. P.; Ribeiro, M. S.; Wainwright, M.; dos Anjos, C.; Sellera, F. P.; Dropa, M.; Nunes, N. B.; Brancini, G. T. P.; Braga, G. U. L.; Arana-Chavez, V. E.; et al. The Biochemical Mechanisms of Antimicrobial Photodynamic Therapy†. *Photochem. Photobiol.* **2023**, *99* (2), 742−750.
(14) Bai, X.; Yang, Y.; Zheng, W.; Huang, Y.; Xu, F.; Bao, Z. Synergistic photothermal antibacterial therapy enabled by multifunctional nanomaterials: progress and perspectives. *Mater. Chem. Front.* **2023**, *7* (3), 355−380.
(15) Xu, Y.; Zhou, W.; Xiao, L.; Lan, Q.; Li, M.; Liu, Y.; Song, L.; Li, L. Bacitracin-Engineered BSA/ICG Nanocomplex with Enhanced Photothermal and Photodynamic Antibacterial Activity. *ACS Omega* **2022**, *7* (38), 33821−33829.
(16) Fan, S.; Lin, W.; Huang, Y.; Xia, J.; Xu, J.-F.; Zhang, J.; Pi, J. Advances and Potentials of Polydopamine Nanosystem in Photothermal-Based Antibacterial Infection Therapies. *Front. Pharmacol.* **2022**, *13*, 829712.
(17) Zhou, Z.; Zhang, L.; Zhang, Z.; Liu, Z. Advances in photosensitizer-related design for photodynamic therapy. *Asian J. Pharm. Sci.* **2021**, *16* (6), 668−686.
(18) Naskar, A.; Kim, K.-S. Friends against the Foe: Synergistic Photothermal and Photodynamic Therapy against Bacterial Infections. *Pharmaceutics* **2023**, *15* (4), 1116.
(19) Ning, L. G.; Liu, P.; Wang, B.; Li, C. M.; Kang, E.-T.; Lu, Z. S.; Hu, X. F.; Xu, L. Q. Hydrothermal derived protoporphyrin IX nanoparticles for inactivation and imaging of bacteria strains. *J. Colloid Interface Sci.* **2019**, *549*, 72−79.
(20) Zhang, A.-N.; Wu, W.; Zhang, C.; Wang, Q.-Y.; Zhuang, Z.-N.; Cheng, H.; Zhang, X.-Z. A versatile bacterial membrane-binding chimeric peptide with enhanced photodynamic antimicrobial activity. *J. Mater. Chem. B* **2019**, *7* (7), 1087−1095.
(21) Awad, M.; Barnes, T. J.; Joyce, P.; Thomas, N.; Prestidge, C. A. Liquid crystalline lipid nanoparticle promotes the photodynamic activity of gallium protoporphyrin against S. aureus biofilms. *J. Photochem. Photobiol., B* **2022**, *232*, 112474.
(22) Plath, A. M. S.; Facchi, S. P.; Souza, P. R.; Sabino, R. M.; Corradini, E.; Muniz, E. C.; Popat, K. C.; Filho, L. C.; Kipper, M. J.; Martins, A. F. Zein supports scaffolding capacity toward mammalian cells and bactericidal and antiadhesive properties on poly(ε-caprolactone)/zein electrospun fibers. *Mater. Today Chem.* **2021**, *20*, 100465.
(23) Liu, T.; Zhang, M.; Liu, W.; Song, X.; Yang, X.; Zhang, X.; Feng, J. Metal Ion/Tannic Acid Assembly as a Versatile Photothermal Platform in Engineering Multimodal Nanotheranostics for Advanced Applications. *ACS Nano* **2018**, *12* (4), 3917−3927.
(24) Chen, Y.; Huang, W.; Dong, Y.; Yu, X.; Mo, A.; Peng, Q. Enhanced Antibacterial Activity of Indocyanine Green-Loaded Graphene Oxide via Synergistic Contact Killing. *Photothermal And Photodynamic Therapy. J. Biomed.Nanotechnol.* **2022**, *18* (1), 185−192.
(25) Liu, Y.; Lan, Q.; Liu, J.; Shi, Y.; Wu, Q.; Wang, Q.; Yang, S.; Cheng, F. Phenylboronic acid-functionalized BSA@CuS@PpIX nanoparticles for enhanced antibacterial photodynamic/photothermal therapy. *J. Drug Delivery Sci. Technol.* **2023**, *88*, 104965.
(26) Gutberlet, B.; Preis, E.; Roschenko, V.; Bakowsky, U. Photothermally Controlled Drug Release of Poly(d,l-lactide) Nanofibers Loaded with Indocyanine Green and Curcumin for Efficient Antimicrobial Photodynamic Therapy. *Pharmaceutics* **2023**, *15* (2), 327.
(27) Miri, M. A.; Habibi Najafi, M. B.; Movaffagh, J.; Ghorani, B. Encapsulation of Ascorbyl Palmitate in Zein by Electrospinning Technique. *J. Polym. Environ.* **2021**, *29* (4), 1089−1098.
(28) Hosseini, F.; Miri, M. A.; Najafi, M.; Soleimanifard, S.; Aran, M. Encapsulation of rosemary essential oil in zein by electrospinning technique. *J. Food Sci.* **2021**, *86* (9), 4070−4086.
(29) Hou, X.; Yang, L.; Liu, J.; Zhang, Y.; Chu, L.; Ren, C.; Huang, F.; Liu, J. Silver-decorated, light-activatable polymeric antimicrobials for combined chemo-photodynamic therapy of drug-resistant bacterial infection. *Biomater. Sci.* **2020**, *8* (22), 6350−6361.
(30) Almeida, A.; Zhao, Z.-J.; Xu, Z.-P.; Ma, Y.-Y.; Ma, J.-D.; Hong, G.; Almeida, A. Photodynamic antimicrobial chemotherapy in mice with Pseudomonas aeruginosa-infected wounds. *PLoS One* **2020**, *15* (9), No. e0237851.

https://doi.org/10.1021/acsomega.4c00180
ACS Omega 2024, 9, 29274−29281